Journal of Computational and Applied Mechanics, Vol. 7., No. 1., (2006), pp. 41–58

NUMERICAL ANALYSIS OF GIANT BRAIN ANEURYSMS

Ferenc Nasztanovics, Brigitta Tóth
Biomechanical Center
Budapest University of Technology and Economics
H-1521 Budapest, Hungary
naszta@biomech.bme.hu, brigitta.toth@index.hu

György Paál, Imre Bojtár
Biomechanical Center, Department of Structural Mechanics
Budapest University of Technology and Economics
H-1521 Budapest, Hungary
paal@vizgep.bme.hu, ibojtar@mail.bme.hu

István Szikora
National Scientific Institute of Neurosurgery
H-1145 Amerikai u. 57.
h13424szi@ella.hu

[Received: September 14, 2004]

Abstract. This paper focuses on the analysis of the haemodynamic pattern and biophysical properties of cerebral aneurysms, diagnosed and delineated in living human individuals. An aneurysm is a bulging out of part of the wall of a blood vessel. The aim of the research is to delineate flow patterns inside the aneurysm and its parent artery, to estimate stresses at critical points of the aneurysm wall, to model the haemodynamic effect of different surgical and endovascular tools in order to define the optimal one in a particular case, and to estimate the likelihood of a later aneurysm rupture.

Keywords: haemodynamic pattern, biophysical properties of cerebral aneurysms

1. **Introduction**

Brain arterial aneurysms are common forms of arterial deformation occurring in about 5% of the adult population. The aneurysm is a bulge along the artery hanging there embedded in the surrounding tissue. In most situations it usually appears around a joining of two arteries. This bifurcation is the part of the supplier of the brain vascular bed system so if its blow-out (rupture) causees an incalculable chain reaction, there is no safe solution without any side-effect to protect the patient against unpleasant consequences, see for instance [1],[2],[3]. In the majority of the cases the patient does not notice anything about the presence of the aneurysm, in some cases, however, the aneurysm bursts leading to stroke and immediate death. Figure 1 presents a photo of an aneurysm obtained by planar angiography, and its characteristic places in the human brain.

At present, the therapeutic decision for unruptured aneurysms is made purely on the basis of the size and location of the lesion in the belief that those are the only

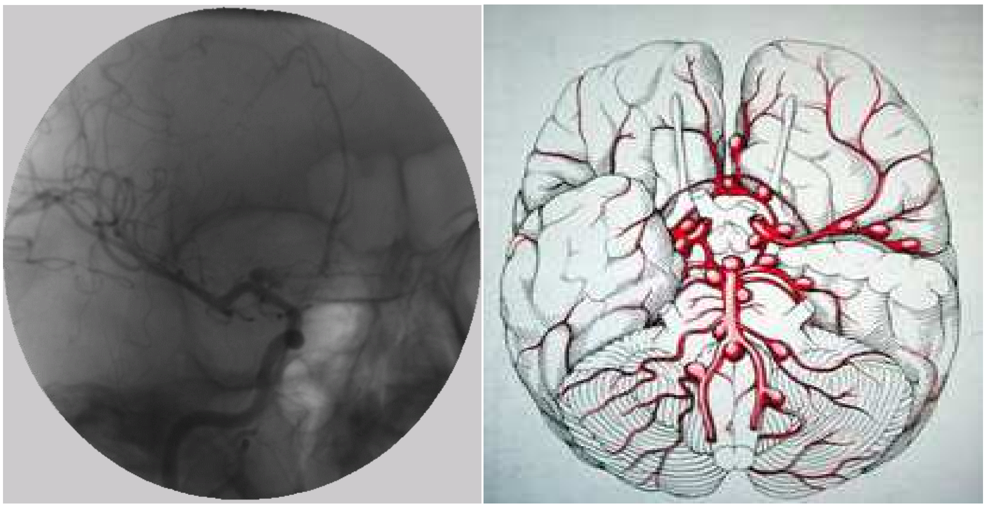

Figure 1. (a) Photo of the aneurysm (b) The usual places where brain anurysm form

factors influencing the likelihood of rupture. The literature results providing a basis for this practice have been seriously criticized by many and clinical decision is frequently based on the personal experience and judgment of the physician. Our work will provide the physicians - and the patients - with a much more accurate prognosis of the disease that will allow for a more appropriate decision regarding treatment. We note that besides its scientific merit, the potential for providing information about the prognosis of the disease and about the optimal technique for its treatment would greatly enhance the value of modern angiography systems.

The description of the flow in arteries (also called haemodynamics,[4],[5],[6]) is one of the great challenges of current fluid mechanics research. The flow is unsteady, the walls are flexible with complex elastic properties, the geometry is very complicated. The living tissue reacts to fluid mechanical changes in unpredictable ways, which again influences the flow properties. The elastic deformation of the wall interacts with the flow in a complex way. The non-newtonian properties of blood also play a role in some cases. There are substantial variations in all the parameters from patient to patient so it is difficult to draw general conclusions. In addition, it is extremely difficult to make in vivo measurements to test theories or simulations.

Nevertheless the importance of this area cannot be overestimated – the most important causes of death in developed countries are arterial diseases. Research budgets and public interest in this subject grow continuously.

2. **Research strategy**

The geometrical and morphological data as well as physiological parameters of the patients collected at the National Institute of Neurosurgery are combined with physiological information of the vessel wall and aneurysm wall provided by the Department of Human Physiology. The calculation of the material parameters of the aneurysm wall there is the first step of our work. Based on this information, the researchers of the Center for Biomechanics prepare 3D coupled (flow and solid) finite element models of the aneurysms. On these models we run strength calculations in order to predict their mechanical strength (allowable blood pressure, etc.), and to compare the effects of different possible medical treatments. This is the second step of the research activity.

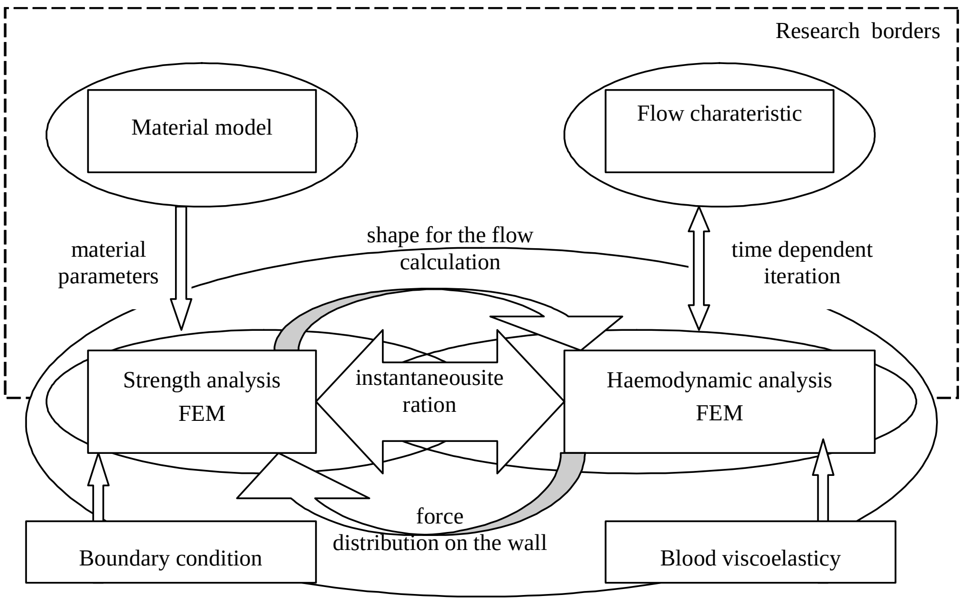

Figure 2. Basic mechanism of the model

The long-term goal of this research program is to work out non-intrusive diagnostic tools detecting the presence of aneurysms and to assess the necessity of medical intervention. To this end detailed studies are being performed on the fluid mechanical behaviour of the blood near aneurisms on the one hand, and on the elasticity behaviour of the blood vessel wall on the other hand. These are performed using commercial software tools.

Since the process is highly unsteady and the elastic deformation of the wall and the flow in the arteries are highly coupled, the solution is far from trivial. After performing simulations on rigid models for fluid mechanics on the one hand and wall only models for the elasticity studies, the next step will be to couple the two phenomena and the data will be transferred in each time step to provide time-dependent boundary conditions for the two simulations.

When the simulations in the realistic model are considered to be reliable the haemodynamic and the wall stress data are carefully analysed and diagnostic criteria for intervention are derived, see Figure 2.

3. Material parameters

3.1. **Introductory remarks.** One of the problems is that the different constitutive models in the literature are based on data from different types of arteries [7],[8],[9]. Moreover, cardiovascular disease like human cerebral aneurysm can only be studied in detail if a reliable constitutive model of the arterial wall is available. In order to get acquainted with the sterically inhomogenous behavior of cerebral aneurysms, we measured the mechanical properties of the aneurysm tissue as a function of strain in different regions (thin and thick) and in different directions (meridional and circumferential). The strips from aneurysm showed typical hyperelastic-plastic behavior at the stress-relaxation tests. Meridional thin strips exhibited greater tensile strenghts than the meridional thick ones, see [10].

Moreover in this point first we have summarized the theoretical framework as a background for the description of the arterial wall mechanics. We begin by giving a brief description of the histological structure of arterial walls and outline the general characteristic of the mechanical response of arteries. An artery is practically treated as a thick-walled circular cylinder which is appropriate for the analysis of bending, extension, inflation and torsion of the tube. In the literature some models are able to provide a full three-dimensional description of the state of stress in the artery, but the large number of material constants may lead to parameter identification problems. Several models use geometrical simplifications as well.

3.2. **Human arterial histology.** In general, arteries are subdivided into two types: elastic and muscular arteries [11],[12]. Elastic arteries have relatively large diameters and are located close to the heart, while muscular arteries are located at the periphery. We focus our attention on the microscopic structure of muscular arterial walls composed of three distinct layers. These are the tunica intima, the tunica media and the tunica adventitia.

The tunica intima is the innermost layer of the artery. A single layer of endothelial cells lines the arterial wall. In healthy young arteries the intima is very thin and does not have any significant contribution to the solid mechanical properties of the human arterial wall. But it is known that pathological changes of the intimal components are associated with significant alterations in the mechanical properties.

The tunica media is the middle layer of the artery and from a mechanical perspective it is the most significant layer. It consists of a complex three-dimensional network of smooth muscle cells and elastin and collagen fibrils. The media is separated by the so-called fenestrated elastic laminae into concentrically fiber-.reinforced layers, and this middle layer is separated from the intima and the adventitia by the internal elastic laminae and the external elastic laminae, respectively. The smooth muscle cells, the elastin and collagen fibrils and the fenestrated elastic laminae constitute a continuous almost circumferentially oriented fibrous helix. This arrangement gives high strength and resilience.

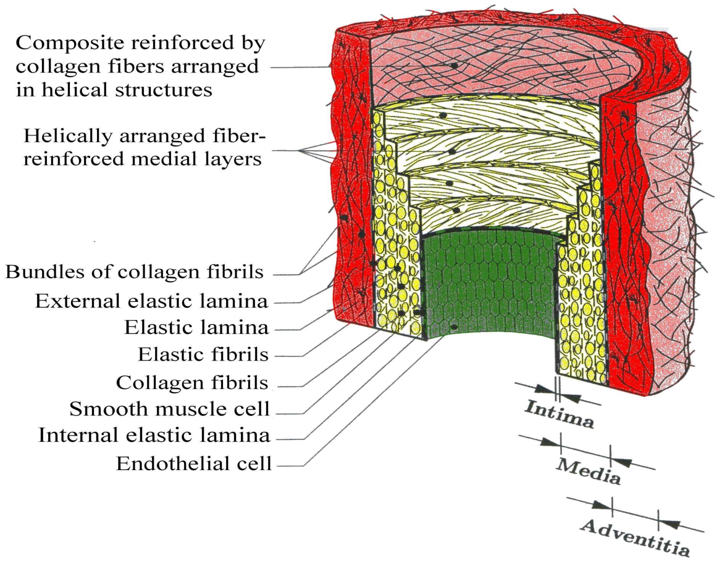

Figure 3. Model of the major components of a healthy artery composed of three layers: intima, media and adventitia

The tunica adventitia is the outermost layer of the artery. The thickness of the adventitia depends on the type of the artery and its topographical site. Apart from a histological ground substance it also consists of fibroblasts, fibrocytes and thick bundles of wavy collagen fibrils, which are arranged in helical structures. They contribute to the strength and stability of the arterial wall. The adventitia is less stiff in a low pressure domain than the media but at higher pressures the collagen fibrils straighten out and the adventitia turns into a stiff tube.

3.3. **Typical mechanical behavior of arterial walls.** The reliability of material parameters is related to the quality of the experimental data [13],[14],[15],[16]. It may come from in vivo tests or from in vitro tests. In in vivo tests the artery is observed under real life conditions, while in vitro tests mimic real loading conditions in a physiological environment. The complex anisotropic material response can only be measured in an in vitro experiment, though the exact physiological circumstances may be rather difficult to simulate.

Arteries do not change their volume in the physiological range of deformation, for this reason they can be regarded as incompressible – rubber-like – materials. Therefore we have set ourselves the task to determine the mechanical properties from biaxial tests: uniaxial extension tests are certainly insufficient to completely quantify the mechanical behavior of arterial walls.

The mechanical behavior of arteries depends on physiological and chemical environmental factors, therefore they were tested in appropriate oxigenated, temperature controlled salt solutions.

Whereas the composition of arterial walls varies along the arterial tree so that the shape of the stress-strain curve for blood vessels depends on the anatomical site, the general mechanical characteristics are the same.

The artery is a heterogeneous system and it can be regarded as a fiber-reinforced composite biomaterial. The layers of the arterial walls are composed mainly of an isotropic matrix material (associated with the elastin) and two families of fibers (associated with the collagen), which are arranged in symmetrical spirals. We note that we have made a simple independent finite element simulation of the biomechanical behavior of the arterial wall to check the effect of the different parameters in different constitutive equations.

3.4. **Continuum-mechanical framework.** Fundamental equations are essential to characterize kinematics, stresses and balance principles, and hold for any continuum body [17]. Generally we use a functional relationship as a constitutive equation, which determines the state of stress at any point x of a continuum body. Our main goal is to study various constitutive equations within the field of solid mechanics appropriate for approximation techniques. We follow the phenomenological approach. It describes the macroscopic behavior of living tissue as continua.

Numerous materials can sustain finite strains without noticeable volume changes. Such types of material can be regarded as incompressible, which is a common idealization in continuum mechanics. Materials which keep the volume constant throughout a motion are characterized by the incompressibility constraint $J = 1$, where J means the determinant of the gradient tensor. In general, these materials are referred to as a constrained materials.

The stress response of hyperelastic materials is derived from the given strain-energy function Ψ:

$$\sigma_{ij} = \frac{\partial \Psi(\varepsilon)}{\partial \varepsilon_{ij}}$$

In the next subsection we summarize the most important energy functions frequently used in biomechanics.

3.5. **Ogden model for incompressible rubber-like materials.** The postulated strain-energy function Ψ describes the changes of principal stretches

$$\Psi = \Psi\left(\lambda_1,\, \lambda_2,\, \lambda_3\right) = \sum_{p=1}^{N} \frac{\mu_p}{\alpha_p}\left(\lambda_1^{\alpha_p} + \lambda_2^{\alpha_p} + \lambda_3^{\alpha_p} - 3\right)$$

where N is a positive integer which determines the number of terms in the strain-energy function, μ_p are constant shear moduli and α_p are dimensionless constants, $p = 1, \ldots, N$. Only three pairs of constants are required to give an excellent correlation with experimental stress-deformation data.

We find after differentiation that the three principal values σ_a of the Cauchy stresses have the form:

$$\sigma_a = -p + \sum_{p=1}^{N} \mu_p \lambda_a^{\alpha_p}, \quad a = 1,\, 2,\, 3$$

where p is a scalar not specified by a constitutive equation. It is to be determined from a boundary condition of the problem considered.

3.6. **Mooney-Rivlin model for incompressible rubber-like materials.** The Mooney-Rivlin model uses the setting $N = 2$, $\alpha_1 = 2$, $\alpha_2 = -2$. Using the strain invariants I_1, I_2 with the constraint condition $I_3 = \lambda_1^2\lambda_2^2\lambda_3^2 = 1$ we obtain that:

$$\psi = c_1\left(\lambda_1^2 + \lambda_2^2 + \lambda_3^2 - 3\right) + c_2\left(\lambda_1^{-2} + \lambda_2^{-2} + \lambda_3^{-2} - 3\right) = c_1\left(I_1 - 3\right) + c_2\left(I_2 - 3\right)$$

with the constants $c_1 = \mu_1/2$ and $c_2 = -\mu_2/2$.

Derivatives of the strain-energy function of the Mooney-Rivlin model with respect to the invariants I_1 and I_2 give the simple associated stress relations:

$$\boldsymbol{\sigma} = -p\mathbf{I} + 2c_1\mathbf{b} - 2c_2\mathbf{b}^{-1}$$

where the strain tensor b^{-1} is the inverse of the left Cauchy-Green tensor $\mathbf{b}$, which is defined by the help of the strain gradient tensor $\mathbf{F}$ as:

$$\mathbf{b} = \mathbf{F}\mathbf{F}^T$$

($\mathbf{F}$ is on the left). It is an important strain measure in terms of spatial coordinates. $\mathbf{I}$ denotes the second-order unit tensor.

3.7. **Neo-Hookean model for incompressible rubber-like materials.** The neo-Hookean model applies the setting $N = 1$, $\alpha_1 = 2$. Using the first principal strain invariant I_1 we find that:

$$\Psi = \mathrm{c}_1\left(\lambda_1^2 + \lambda_2^2 + \lambda_3^2 - 3\right) = c_1\left(I_1 - 3\right)$$

with the constant $c_1 = \mu_1/2$. The strain-energy function involves a single parameter only and relies on phenomenological considerations.

Derivatives of the strain-energy function of the neo-Hookean model with respect to the invariants I_1 give the simple associated stress relations:

$$\boldsymbol{\sigma} = -p\mathbf{I} + 2c_1\mathbf{b}\ ,$$

where the strain tensor $\mathbf{b}$ is the left Cauchy-Green tensor, and $\mathbf{I}$ is the unit tensor.

3.8. **Some other constitutive models for arterial walls.** We note that in the literature other versions could be found for the constitutive equations of human artery walls, see for instance works by Delfino, Vaishnav, Fung [19] and especially Holzapfel [13],[18]. In these models the active mechanical behavior of arterial walls is governed mainly by the intrinsic properties of elastin and collagen fibers and by the degree of activation of smooth muscles, however the passive mechanical behavior is quite different and is governed mainly by the elastin and the collagen fibers. Most constitutive models describe the artery as a macroscopic system and capture the response near the physiological state.

In our program – based on our laboratory tests – we applied the most common strain-energy functions, mentioned above in Subsections 3.2-3.7. In Figure 4 our uniaxial and biaxial test machines can be seen, both of them are connected to the computer. In our recent numerical simulations the test results of the biaxial specimens were not applied yet, because of the yet insufficient number of experimental results.

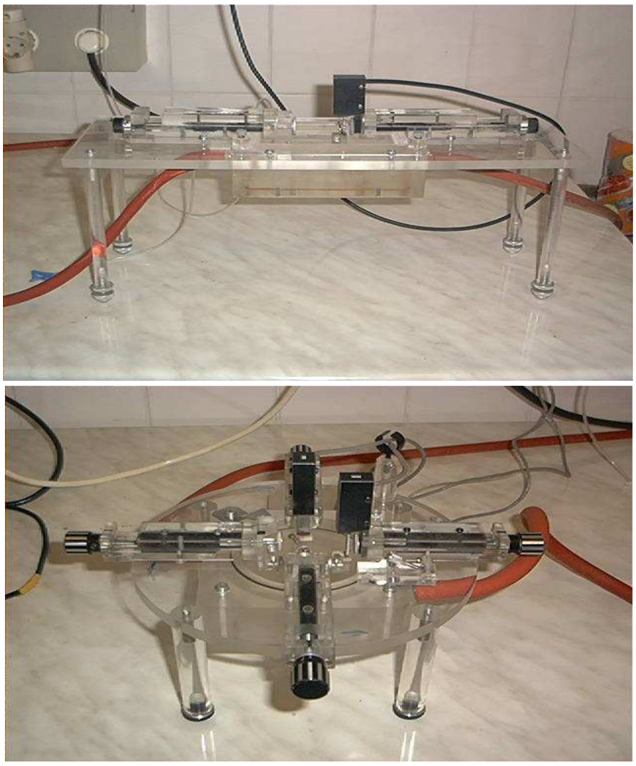

Figure 4. Uniaxial and biaxial laboratory test machines

In Figure 5 we show some characteristic experimental diagrams. We had 53 different specimens from 30 persons. All tests were made immediately after the operations, within 24 hour intervals. Meridian and circumferential strips were cut and measured from the aneurysma sack.

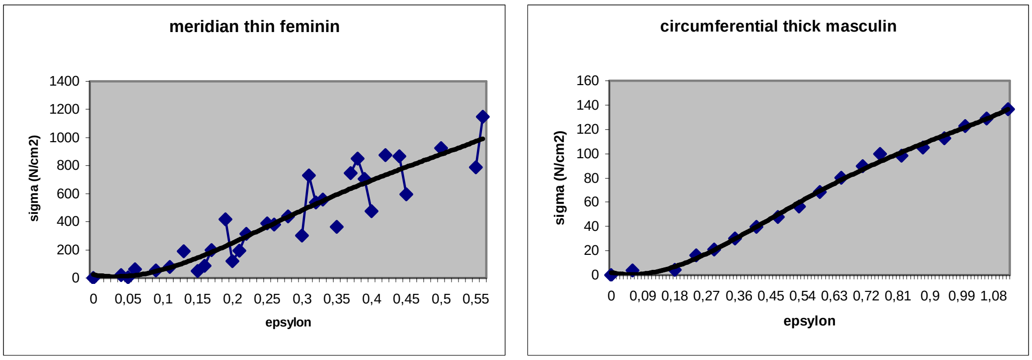

Figure 5. Diagram of an uniaxial stress-strain curve for meridian and circumferential aneurysma strip in passive condition (based on tests performed in the authors' laboratory). The thick solid line indicates the approximate engineering response of the biomaterial.

Based on these experiments we calculated the material parameters of the Mooney-Rivlin and Neo-Hooke nonlinear hyperelastic models, see Table 1. With the help of simple finite element tests all material parameters were checked.

Table 1. Mooney-Rivlin and Neo-Hooke material parameters calculated from experiments

	Mooney-Rivlin				**Neo-Hooke**	
	C10	**C10**	**C01**	**C01**	**C10**	
	Woman	*Man*	*Woman*	*Man*	*Woman*	*Man*
circumferential-thick	5,2	1,6	1,3	0,4	6,5	2,0
circumferential-thin	17,9	14,4	4,5	3,6	22,4	18,0
Meridian-thick	8,7	6,5	2,2	1,6	10,9	8,1
Meridian-thin	22,3	20,3	5,6	5,0	27,9	25,3

4. **Flow simulations**

4.1. **How to simulate.** The simulations were carried out using the commercial flow simulation software CFX 5.6. It solved the incompressible unsteady Navier-Stokes equations using the finite volume method. The fluid had a constant density of 1050 kg/m^3 and a dynamic viscosity of 0.003 kg/ms so that the non-newtonian behavior of blood was ignored. The simulations were performed on the simplified model introduced in [5]. Figure 6a shows that the aneurysm head sitting on a pipe bifurcation is inclined so that it stands out of the plane of the pipes. In order to have well-defined boundary conditions, the original geometry was extended by straight pipe sections (Figure 6b).

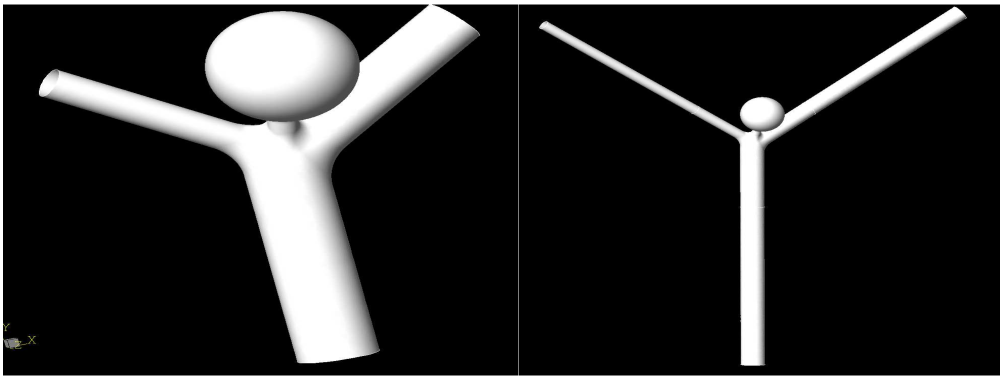

Figure 6. (a) Model of idealized aneurysm geometry (b) Extended geometry

The simulated volume was divided into about 200.000 mainly tetrahedral elements, except near the walls, where prismatic elements were used to achieve better boundary layer resolution. The wall was assumed to be rigid and standard no-slip boundary condition was used with automatic near-wall treatment. The mesh was made significantly finer in regions of high curvature, i. e. near the aneurysm neck.

The inlet boundary condition was an analytic mass flow rate-time function resembling a real blood pulse cycle (Figure 7). Two cycles were simulated and the second one was used to extract results. The extension on the inlet pipe was used in order to be able to use a uniform inlet velocity profile and not to interfere with the flow developing later.

At a later stage of the project the inlet boundary condition will be derived directly from ultrasonic velocity measurements in real patient arteries. These signals are at present very noisy and require filtering and smoothing in order to use them in simulations.

The outlet boundary condition presents an interesting problem. A time-dependent boundary condition cannot be given, since the time delay and the deformation of the pulse passing the aneurysm region cannot be said a priori. On the other hand, far away from the artery, on the level of capillaries, the pressure reaches a nearly constant value. Therefore a constant pressure outlet boundary condition was used and all the blood vessels lying between the region of interest and the region of constant pressure have been simulated by a pipe section filled with "porous material". This had the function to dissipate the pressure variations and arrive at a constant pressure in the end.

The time period was divided into twenty equal time steps and this time step was used for the simulation. The temporal discretisation as well as the spatial discretisation were second order.

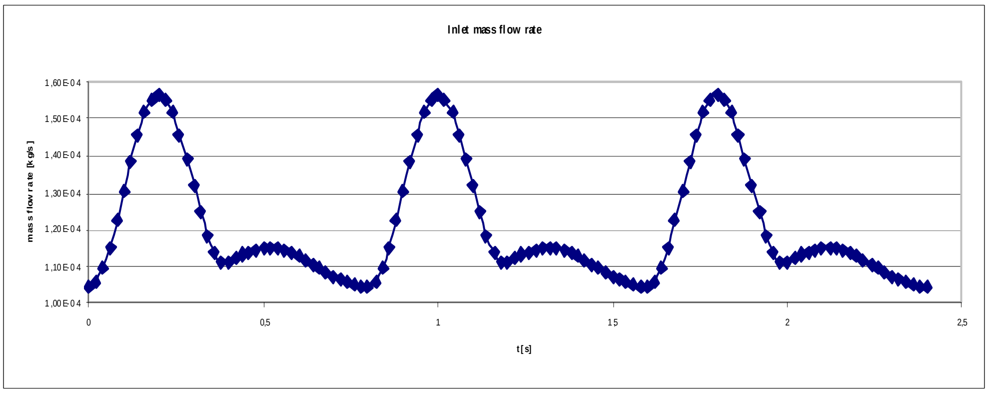

Figure 7. Inlet boundary condition

4.2. **Results of the idealized geometry.** Some preliminary results are shown to demonstrate the capabilities of the simulations. This idealization may be far from the real aneurysm but it is simple enough for testing the model behavior. The idealized

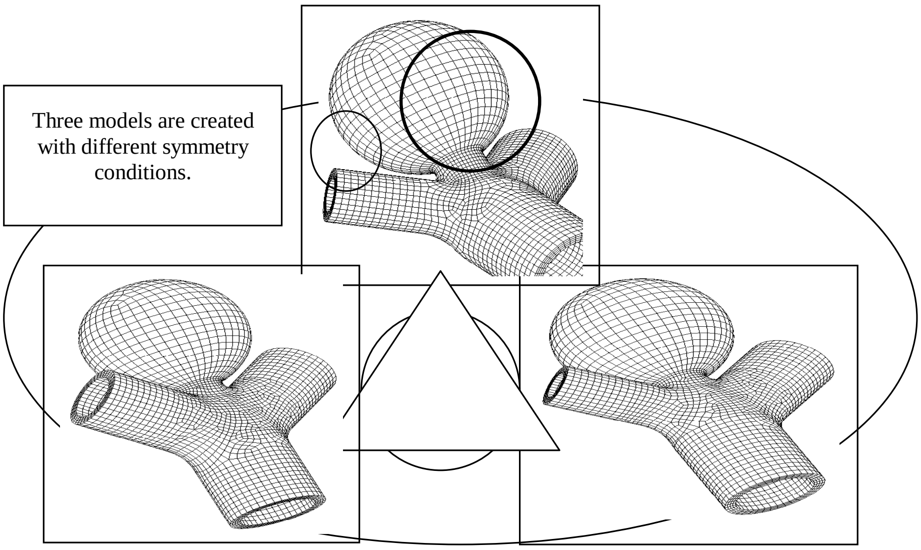

Figure 8. Different ideal geometries

model is built up of three cylinders and a sphere skew penetration. The bottom cylinder is the inflow pipe, and the two others are the outflow. Three different types of penetration were applied. The angle and the diameter of the cylinders were changed.

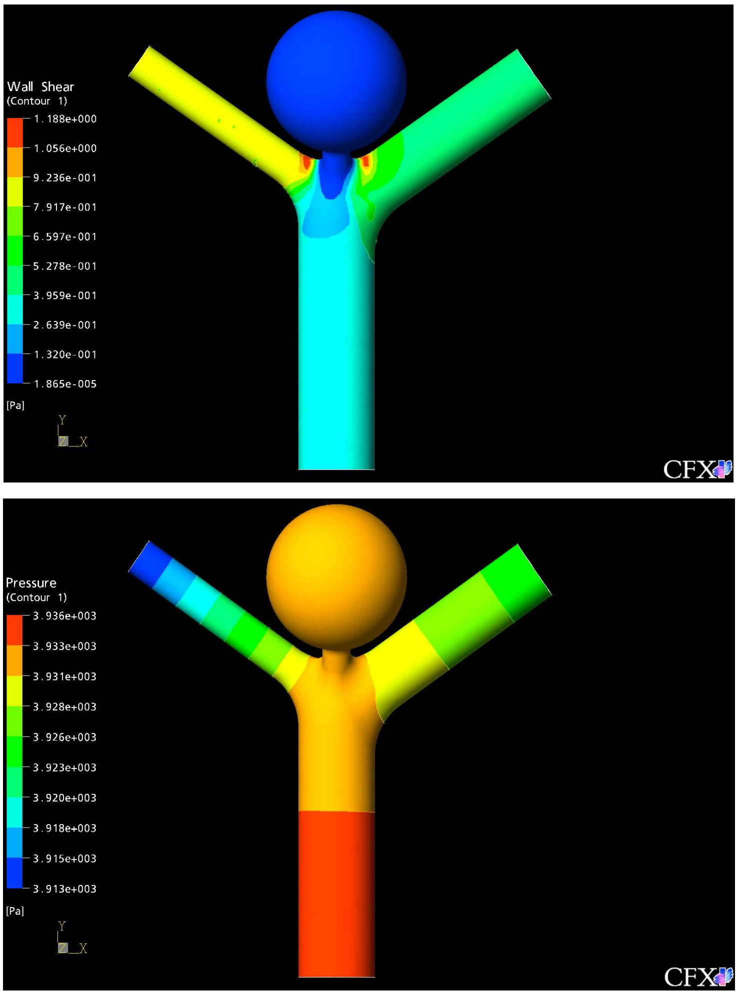

Figure 9. Wall shear stress and pressure distribution along the aneurysm walls

All the figures shown are from an arbitrary time step, practically at the peak systole. Results in all the other time steps look qualitatively similar, only the magnitudes of the variables change significantly.

Figure 9a shows the wall shear stress. In the aneurism 'bulge' itself the shear is negligible, which is a consequence of the negligible flow velocities there (not shown in the paper). In the incoming and outgoing pipes the shear stress is constant. Note that higher wall shear values can only be detected at the 'shoulders' of the aneurysm.

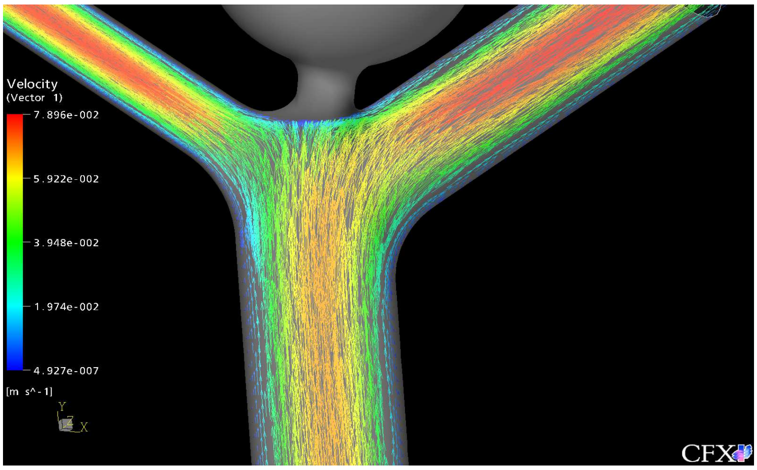

Figure 10. Blood velocity vector field in the model mid-plane

This, however cannot be the cause of the rupture since experience shows that it usually happens along the 'equator' of the aneurysm.

The wall pressure distribution (Figure 9b) shows the expected linear decrease in the pipe regions and a practically constant value in the aneurysm region. It is expected that a better model provides here more information.

Finally the velocity distribution (Figure 10) also presents no dramatic phenomena. The flow is smooth, well-behaved, without any vortices and separations. A more refined model is expected to reveal more anomalies here as well.

4.3. **Results of the real geometry.** With the help of angiography we can build a model of an existent aneurysm, and this model was used for Finite Element Analysis calculation. The angiography allows us to build a real three dimensional model with the original geometry. Using the data of aneurysm material parameters the system could help the physicians to analyze the case, whether it needs an urgent operation or not. This way of geometrical modeling is much more complicated than the previous one. Many different tests are needed to declare that the system works reliably. Moreover, different material models and boundary conditions need more and more calculations. On this part of the task we have just started to work. The system is almost ready for the final testing. Thanks to the engineers of General Electric, we are able to gain three dimensional geometrical data from angiography

At this moment we analyzed two real aneurysm sacks with similar boundary and load conditions as were made in the idealized situations. In Figure 11 the velocities at the moment of the peak systole can be seen. We note that in the second situation – following from the geometry of the aneurysm - the velocity in the sack is smaller than in the first case.

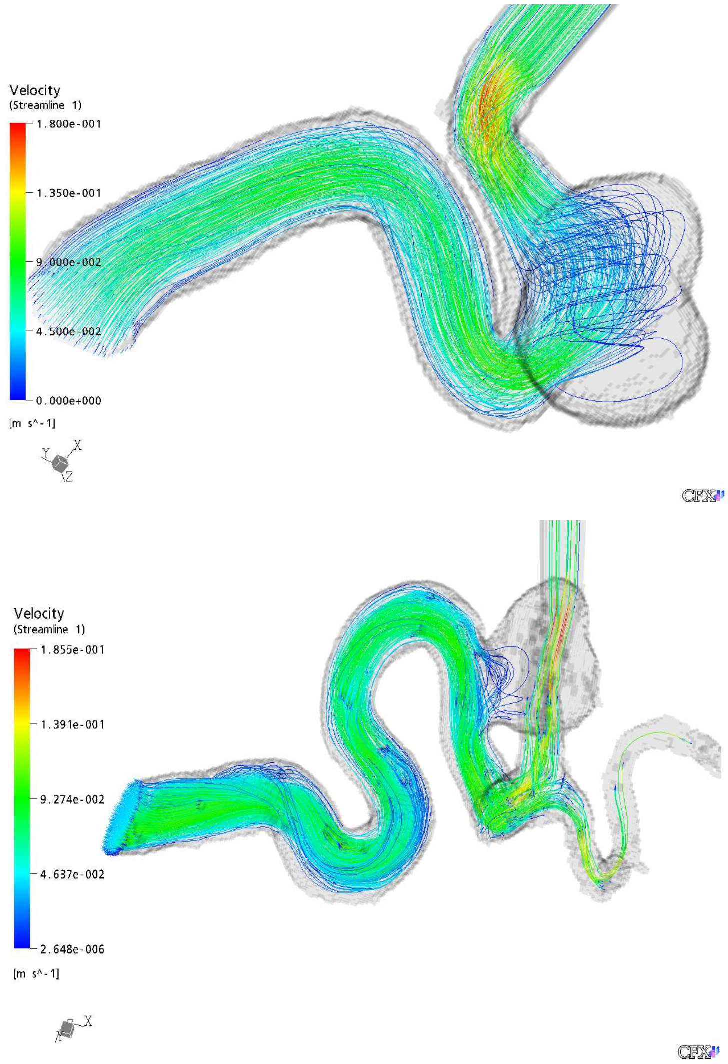

Figure 11. Stream lines in two different aneurysms

The shear stresses could be seen in Figure 12 for these aneurysm sacks. In both situations there are relatively small shear stresses at the internal surface of the balloons.

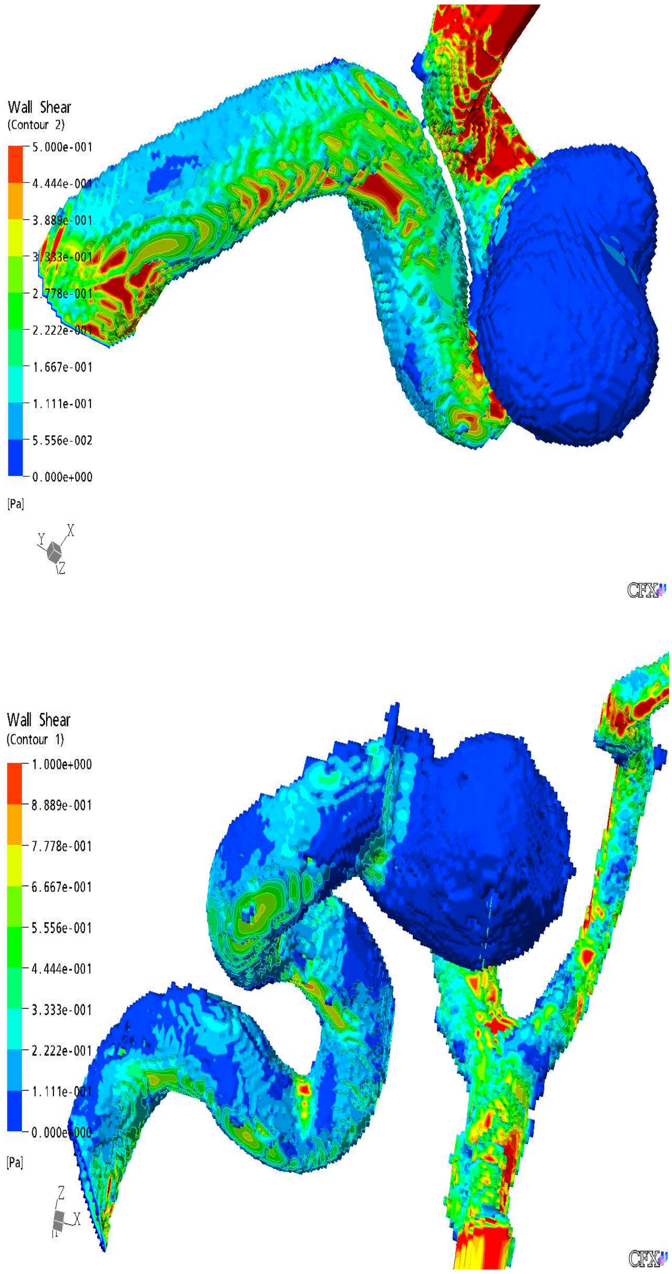

Figure 12. Shear stresses at the internal surfaces of the walls

5. Analysis of the artery wall

The task is to give an approximate computation for the stress changing in the wall caused by the changing of the haemodynamics, surroundings, and wall material. The resource assimilates the study of vascular material changing after evolution of brain aneurysm based on laboratory experiment. The haemodynamical behaviour (contrary to the original state) has definitely changed because of the large local displacements. In this case the bloodstream is interpreted as a function of the wall shape.

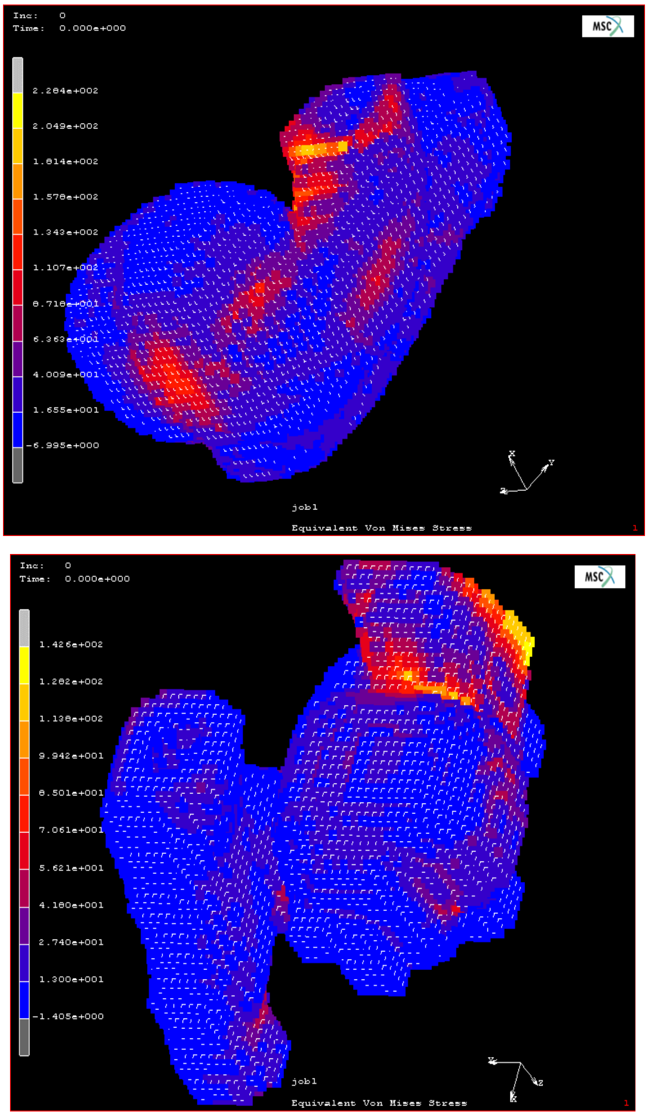

Figure 13. Mises-stresses in the walls of different aneurysms

On the other hand, the shape of the vascular wall is defined by the surroundings and the haemodynamics itself. Therefore all haemodynamical calculations should be done with the help of the current shape of the vascular system.

So far it seems that only one of the two tasks can be solved at a time. This means that the forces expressed by the haemodynamical behavior change the stress distribution inside the wall. Using the stress distribution change and complex material model, the increase in deformation (field of strain) can be calculated. Because this deformation is usually large, so all the calculations have to be done on the changed geometry, not on the original. That is why all the numerical calculations are geometrically nonlinear.

The original aneurysm is taken out from its environment in our approach, and it is analyzed in itself, with the help of numerical methods and connected boundary conditions. This shortcut does not cause large errors in the model. This point is related to the strength analysis so the task is to estimate the stress distribution due to the forces given by the haemodynamical analysis, boundary conditions, and the applied material model. Two different types of geometry were tested during the research: first we used an idealized model to adjust the model parameters and assay the effect of the change of the model; the second type of geometrical data were gained from angiography results.

The well-known finite element method was applied as a numerical approximation for these two different systems. We used MSC Marc and Ansys for both strength calculations. Figure 13 shows the details of the calculated wall-stresses at the maximum systole pressure in the real geometry.

6. **Summary**

In cooperation with the staff of the National Institute of Neurosurgery and Human Sciences we made the first steps in the complex numerical simulations of brain aneurysms. Our connected system can calculate the dynamic flow parameters of blood and from this effect can determine the displacements and stresses in the vessel wall. In the future we plan to continue our work by refining the finite element mesh and then we want to simulate the load bearing capacity of the rupturing balloon of the aneurysm sack.

Acknowledgement. This work was done with the help of an OTKA-grant (leader dr. István Szikora, National Institute of Neurosurgery).

REFERENCES

1. Thubrikar, M.J.: Wall stress studies of abdominal aortic aneurysm in a clinical model., *Annals of vascular surgery*, **15**, (2001), 355-366.
2. Lermusiaux, P., Leroux, C., etc.: Aortic aneurysm: construction of a life-size model by rapid prototyping. *Annals of vascular surgery*, **15**, (2001), 131-135
3. Steinman, D.A., etc.: Image-based computational simulation of flow dynamics in a giant intracranial aneurysm.*American J. of Neuroradiology*, **24**, (2003), 559-566.

4. Fung, Y. C.: *Biomechanics: Circulation.* Springer, New York, 1997.
5. Liepsch, D.: An introduction to biofluid mechanics – basic models and applications. *J. of Biomechanics*, 35, (2002), 415-435.
6. Egelhoff, C.J., etc.: Model studies of the flow in abdominal aortic aneurysm during resting and exercise conditions. *J. of Biomechanics*, **32**, (1999), 1319-1329.
7. O'Rourke M.F.: Vascular mechanics in the clinic. *J. of Biomechanics*, **36**, (2003), 623-630.
8. Choung, C.J. and Fung, Y.C.: Three-dimensional stress distribution in arteries. *J. Biomech. Engr.*, **105**, (1983), 268-274
9. Vorp, D.A., Rajagopal, K.R., Smolinsky, P.J. and Borovetz, H.S.: Identification of elastic properties of homogeneous orthotropic vascular segments in distension. *J. Biomech.*, 28, (1995), 501-512.
10. Tóth, M., Nádasy, G.l., Nyáry, I., T. Kerényi, T., Orosz, M., Molnárka, G. and Monos, E.: Sterically inhomogeneous viscoelastic behavior of human saccular cerebral aneurysms. *J. Vasc. Res.,* **35**, (1998) 345-355.
11. Fonyó, A.: *Textbook of Medical Physiology.* Medicina, Budapest, 1999. (in Hungarian)
12. Mónos, E.: Hemodynamics: dynamics of the blood circulation. Lecture notes, Budapest, 2001. (in Hungarian)
13. Holzapfel, G.A., Gasser, T.C. and Ogden, R.W.: A new constitutive framework for arterial wall mechanics and a comparative study of material modes. *Journal of Elasticity,* **61**, (2000), 1-48.
14. Finlay, H.M., McCullough, L. and Canham, P.B.: Three-dimensional collagen organization of human brain arteries at different transmural pressures. *J. Vasc. Res.*, **32**, (1995), 301-312.
15. Weizsäcker, H.W. and Pinto, J.G.: Isotropy and anisotropy of the arterial wall. *J. Biomech.*, **21**, (1988), 477-487.
16. Rhodin, J.A.G.: Architecture of vessel vall. In Sparks, H.V. Jr., Bohr, D.F., Somlyo A.D. and Geiger, S.R., editors, Handbook of Physiology, The Cardiovascular System II. 1-31. American Physiologial Society, Bethesda, Maryland, 1980.
17. Silver, F.H., Christiansen, D.L. and Buntin, C.M.: Mechanical Properties of the Aorta: *Critical Rewiews in Biomed. Engr.*, 17, (1989), 323-358.
18. Holzapfel, G.A.: Nonlinear Solid Mechanics. A Continuum Approach for Engineering. John Wiley & Sons, Chichester, 2000.
19. Fung, Y. C.:. *Biomechanics: Mechanical Properties of Living Tissue.* Springer-Verlag, New York, 2. ed., 1993